Tandem amplification of SCCmec can drive high level methicillin resistance in MRSA

AAC00869-17 REVISED

Tandem amplification of SCC*mec* can drive high level methicillin resistance in MRSA

Laura A. Gallagher[1], Simone Coughlan[2,3], Nikki S. Black[1], Pierce Lalor[1], Elaine M. Waters[1], Bryan Wee[2], Mick Watson[2], Tim Downing[3], J. Ross Fitzgerald[2], Gerard T. A. Fleming[1]* and James P. O'Gara[1]*

[1]Department of Microbiology, School of Natural Sciences, National University of Ireland, Galway, Ireland.

[2]School of Mathematics, Statistics and Applied Mathematics, National University of Ireland, Galway, Ireland.

[3]School of Biotechnology, Dublin City University, Dublin 9, Ireland.

[4]Roslin Institute, The University of Edinburgh, Scotland, UK.

***Correspondence:**

James P. O'Gara: jamesp.ogara@nuigalway.ie

Gerard T. A. Fleming: gerard.fleming@nuigalway.ie

Key words: *Staphylococcus*; SCC*mec*; beta-lactam; antibiotic; resistance; mechanism

Running title: Amplification of SCC*mec* is a new mechanism of high level β-lactam resistance in MRSA

Abstract. Hospital-associated methicillin-resistant *Staphylococcus aureus* strains typically express high level, homogenous (HoR) β-lactam resistance, whereas community-associated MRSA (CA-MRSA) more commonly express low level heterogeneous (HeR) resistance. Expression of the HoR phenotype typically requires both increased expression of the *mecA* gene, carried on the *Staphylococcus* cassette chromosome SCC*mec* element, and additional mutational event(s) elsewhere on the chromosome. Here the oxacillin concentration in a chemostat culture of the CA-MRSA strain USA300 was increased from 8 µg/ml to 130 µg/ml over 13 days to isolate highly oxacillin resistant derivatives. A stable, small colony variant, designated HoR34, which had become established in the chemostat culture was found to have acquired mutations in *gdpP, clpX*, *guaA* and *camS*. Closer inspection of the genome sequence data further revealed that reads covering SCC*mec* were ~10 times over-represented compared to other parts of the chromosome. qPCR confirmed >10-fold higher levels of *mecA* DNA on the HoR34 chromosome, and MinION genome sequencing verified the presence of 10 tandem repeats of the SCC*mec* element. qPCR further demonstrated that sub-culture of HoR34 in varying concentrations of oxacillin (0–100 µg/ml) was accompanied by accordion-like contraction and amplification of the SCC*mec* element. Although slower growing than USA300, HoR34 out-competed the parent strain in the presence of sub-inhibitory oxacillin. These data identify tandem amplification of the SCC*mec* element as a new mechanism of high-level methicillin resistance in MRSA, which may provide a competitive advantage for MRSA under antibiotic selection.

45 **Introduction**

46 In recent decades, the overall incidence of methicillin resistant *Staphylococcus aureus*
47 infections has greatly increased due to the emergence of community-associated MRSA (CA-
48 MRSA), which are increasingly displacing hospital associated-MRSA (HA-MRSA) strains in
49 healthcare settings (1). Methicillin resistance is mediated by the *mecA*-encoded low affinity
50 penicillin binding protein 2a carried on the mobile *Staphylococcus* cassette chromosome
51 *mec* element (SCC*mec*). Heterogeneity is a feature of *S. aureus* methicillin resistance (2). In
52 general clinical CA-MRSA isolates exhibit low level, heterogeneous methicillin resistance
53 (HeR) under laboratory growth conditions, whereas HA-MRSA isolates can exhibit high-level,
54 homogeneous methicillin resistance (HoR). HeR strains can express a HoR phenotype after
55 selection on elevated concentrations of β-lactam antibiotics, via mechanism(s) involving the
56 stringent response and altered c-di-AMP signalling (2).
57 In general, the capacity of pathogens like MRSA to become resistant to new drugs only
58 becomes apparent months or years after their introduction into clinical practice, during
59 which time exposure of the pathogen to new drugs gradually increases, as does the
60 likelihood that endogenous resistance will emerge. This clinical scenario can be mimicked in
61 the laboratory using standard, batch culture techniques to isolate bacterial mutants
62 exhibiting resistance to an antimicrobial drug. However, such artificial culture conditions can
63 mask the impact of acquired antimicrobial resistance (AMR) on bacterial fitness (3, 4), a
64 phenomenon that plays a significant role in determining maintenance and spread of the
65 AMR genotype in natural bacterial populations, and affects the disease-causing capacity of
66 the pathogen. Here we used a continuous-growth chemostat to address this limitation by
67 creating a more dynamic and competitive environment from which to isolate
68 physiologically-relevant β-lactam resistant mutants. A USA300 culture was exposed to

69 increasing concentrations of oxacillin (8-130 μg/ml) over a thirteen-day period. Among the
70 hyper-resistant mutants isolated was a stable small colony variant in which the tandem
71 amplification of the SCC*mec* element was identified as a new mechanism of high-level β-
72 lactam resistance in MRSA.

Results and discussion

Isolation of USA300 oxacillin hyper-resistant mutants. A USA300 nutrient broth culture was grown in a chemostat for 13 days. A sub-MIC concentration of oxacillin was used at the start of the chemostat culture and increased on an incremental, daily basis up to 130 μg/ml (equivalent to 800 μg/ml on Mueller Hinton, BHI or nutrient agar), as described in the methods. Isolated hyper resistant mutants were readily differentiated into i) white coloured small colony variants and ii) regular-sized, pigmented colonies (Fig. 1A). Using population analysis profiling as described previously (5), all the mutants were shown to be homogeneously resistant (HoR) (data not shown) and exhibited oxacillin MICs = 800 μg/ml. Further analysis revealed that the small colony mutants appeared to be phenotypically similar, exhibiting the same biofilm forming capacity and repressed β-haemolysis (data not shown). In contrast the faster growing HoR mutants appeared to be heterogeneous, exhibiting different levels of biofilm forming capacity and β-haemolytic activity on sheep blood agar (data not shown). Whole genome sequencing further revealed a variety of different mutations in nine HoR mutants recovered from the chemostat (Table 1). These included four mutants with $Ser_{67}Lys$ amino acid substitutions in DacA, the diadenylate cyclase responsible for synthesis of c-di-AMP, which has previously been implicated in the HoR phenotype (2, 6, 7), four mutants with five different mutations in genes encoding predicted lipoproteins and one mutant with a $Glu_{227}Gln$ substitution in a predicted ABC transporter designated *abcA* (8). Mutation of the *abcA* gene has previously been shown to increase β-lactam resistance and is associated with upregulation of the adjacent *pbpD* gene, which encodes penicillin binding protein 4 (8).

95 In addition to a small colony size (Fig. 1A), impaired growth (Fig. 1B) and expression of
96 hyper-resistance to oxacillin, a representative SCV HoR, designated HoR34, also exhibited
97 altered cell morphology including defective septa formation (Fig. 1C) and an approximately
98 2-fold increase in cell wall thickness (18.6 ± 1.8 nm in USA300 versus 36.1 ± 4.2 nm in
99 HoR34)(Fig. 1D). Whole genome sequence analysis of HoR34 and the parent USA300 strain
100 compared to the publically-available USA300 FPR3757 genome, revealed that plasmid
101 pUSA02 (which carries tetracycline resistance) had been lost and identified non-
102 synonymous mutations in the *gdpP* (c-di-AMP phosphodiesterase (2, 7)), *guaA* (GMP
103 synthetase (9)), *clpX* (chaperone protein (10)) and *camS* (membrane lipoprotein (11)) genes
104 (Table 1). GdpP is an c-di-AMP phosphodiesterase responsible for turnover of c-di-AMP
105 synthesised by DacA, and has previously been implicated in the HoR phenotype (2, 7) but
106 not a small colony phenotype, which is clinically important in persistent infections (12).
107 Therefore to determine if the *guaA*, *clpX* or *camS* mutations (alone or in combination) were
108 involved in the small colony size of HoR34, the mutant was subjected to daily subculture in
109 the absence of antibiotic selection for 2 weeks in an effort to isolate fast-growing
110 revertants. The SCV phenotype of HoR34 was stable and no fast growing revertants were
111 isolated even after repeated attempts. However the oxacillin MIC of the passaged HoR34
112 strain, designated HoR34p, was reduced from 800 μg/ml to 300 μg/ml, indicating that
113 although the strain continued to be hyper-resistant, oxacillin resistance levels in this strain
114 can be regulated.
115 To further tease out the contributions of the *guaA, clpX, camS and gdpP* mutations to the
116 HoR34 phenotypes, wild type alleles of the four genes, including their upstream promoter
117 sequences, were cloned on the medium copy number *E. coli-Staphylococcus* shuttle plasmid
118 pLI50 and introduced into HoR34. The multicopy *clpX* plasmid was unstable in HoR34 and

rapidly lost in the absence of antibiotic selection. Furthermore imposition of continuous antibiotic selection for the p*clpX* plasmid in HoR34 appeared to be accompanied by the selection of compensatory mutations, as evidenced by the rapid emergence of fast growing colonies among the HoR34 small colony variants. Although we were unable to progress this complementation experiment further, two previous studies have shown that mutation of *clpX* is associated with increased resistance to β-lactam antibiotics (albeit not to the levels measured in HoR34) (10, 13), suggesting that the *clpX* mutation may contribute in part to increased oxacillin resistance in HoR34. The remaining complementation experiments revealed that neither *gdpP*, nor the *camS* and *guaA* genes had any significant effect on the colony morphology (data not shown) or oxacillin MIC of HoR34, as measured by Etest (Fig. 2A) and agar dilutions (data not shown). Furthermore, the doubling times for HoR34 (31.9 min), HoR34 p*guaA* (33.0 min), HoR34 p*gdpP* (31.7 min) and HoR34 p*camS* (28.9 min) were all substantially slower than USA300 (22.6 min) and HoR34 grown in Ox 0.5 μg/ml (32.70 min), but not significantly different from each other indicating that the *guaA, camS and gdpP* mutations alone did not affect growth rate. Because GdpP and c-di-AMP signalling also contributes to the regulation of autolytic activity (2, 14), we further investigated this phenotype. Consistent with previous studies, the *gdpP* mutation in HoR34 was associated with increased autolytic activity that was successfully complemented only by *gdpP* and not *camS* or *guaA* (Fig. 2B). The potential roles of the identified mutations in *guaA, clpX* and *camS* in the HoR phenotype remain unclear but they may have emerged initially to support growth or maintain fitness at relatively lower oxacillin concentrations during the early stages of growth in the chemostat. It seems unlikely that the mutations in *camS, clpX* or *guaA* are accompanied by any gain of function; the *clpX* and *camS* genes contain mutations introducing stop codons (Table 1), while predicted loss of function mutations in *guaA* have

143 previously been implicated in the HoR phenotype (7). Taken together, these data suggest
144 that the mutations in *guaA, clpX, camS and gdpP*, at least on their own, are not responsible
145 for the HoR34 oxacillin hyper-resistance phenotype, and raised the possibility that other
146 genomic rearrangements were responsible for this phenotype.

147 **Chromosomal amplification of the SCC*mec* element in HoR34**. A number of recent studies
148 have indicated that large regions of the *S. aureus* chromosome can undergo duplication and
149 amplification events (15, 16). To investigate if such genomic rearrangements had taken
150 place in HoR34, read coverage across the genome was analysed. Illumina sequence reads
151 covering the SCC*mec* element were >10 times over-represented compared to other parts of
152 the chromosome (Fig. 3). LightCycler qPCR confirmed 10-fold higher levels of *mecA* in HoR34
153 gDNA samples compared to USA300 (data not shown). To determine whether the SCC*mec*
154 element had amplified on the chromosome or excised and re-integrated at multiple sites
155 around the chromosome, we attempted to assemble the Illumina sequence reads
156 corresponding to the SCC*mec* element into contigs. However these efforts were hampered
157 by the short reads. To address this we re-sequenced the HoR34 genome using MinION
158 technology, which generates sequence reads of 10Kb onto which the Illumina sequence
159 reads were mapped. The combined MinION/Illumina sequence data revealed the presence
160 of 10 tandem SCC*mec* element repeats on the HoR34 chromosome (Fig. 4). All 10 copies of
161 SCC*mec* were completely intact and no additional DNA sequences were identified at the join
162 sites. Oligonucleotide primers designed to span the join sites of tandem SCC*mec* elements
163 amplified PCR produced of the predicted size from HoR34 but not USA300, whereas control
164 primers targeting *mecA* amplified PCR products of the predicted size from both HoR34 and
165 USA300 (Fig. 5A).

Stability of the SCC*mec* amplification event. The reduction in oxacillin MIC in the HoR34 strain passaged in BHI media (from 800 to 300 μg/ml) indicated that the amplified SCC*mec* elements may be unstable in the absence of antibiotic selection. To measure SCCmec copy number, LightCycler qPCR was used to compare the relative abundance of *mecA* in HoR34 grown in the presence and absence of oxacillin. These experiments revealed that the *mecA* copy number in the HoR34p strain that had been passaged daily in antibiotic-free BHI media for 2 weeks (oxacillin MIC = 300 μg/ml), was only 3-fold higher than USA300 (Fig. 5B), indicating that up to seven of the amplified SCC*mec* elements were excised/lost from the original chemostat isolate during this time. Interestingly the doubling time of HoR34p (32.70 min) was not significantly different to that of HoR34 (31.9 min), indicating that a reduction in the number of amplified SCC*mec* elements was not sufficient to alleviate the growth defect. However further passage of HoR34p in 0.5, 64 and 100μg/ml oxacillin was accompanied by a significant, concentration-dependent increase in *mecA* copy numbers (up to 17-fold compared to USA300)(Fig. 5B), and an increase in MIC to ≥800 μg/ml. PCR amplification and sequencing was used to confirm that the identified mutations in the *guaA, gdpP, clpX and camS* genes of HoR34 had not reverted to wild type following passage in antibiotic free media (data not shown). These data suggest that recombination between the tandem SCC*mec* elements in HoR34 facilitates accordion-like contraction and expansion in response to oxacillin exposure. Consistent with these qPCR data, Western blot analysis of HoR34 grown in 0, 0.5, 64 and 100 μg/ml oxacillin also revealed concentration-dependent increases in PBP2a expression (Fig. 5C).

To investigate why a small colony variant may have been selected and maintained in the chemostat, we performed competition experiments between USA300 and HoR34. Predictably USA300 out-competed the slower-growing HoR34 in the absence of antibiotic

selection (Fig. 5D). However in the presence of sub-inhibitory oxacillin (0.5 μg/ml), HoR34 strongly outcompeted the wild type (Fig. 5D). Collectively these data identify tandem amplification of the SCC*mec* element as a new mechanism of high-level methicillin resistance in MRSA, which may provide a competitive advantage for MRSA under antibiotic selection.

Concluding remarks. Several genetic mechanisms may have contributed alone or in combination to the SCC*mec* amplification event in HoR34. Expression of the *ccr* recombinase genes which excise SCC*mec* (17) can be increased by β-lactams and vancomycin (18), potentially generating multiple, extrachromosomal copies of SCC*mec* capable of subsequent reintegration. This possibility is supported by a recent study which identified a replication initiator gene upstream of the *ccr* recombinase genes suggesting that the element may be replicative (19). Other mechanisms that may have contributed to the SCC*mec* amplification, alone or in combination with Ccr-mediated excision, include RecA-dependent non-equal homologous recombination or RecA-independent mechanisms such as recombination between single-stranded repetitive sequence on sister chromatids at the replication fork (20). The absence of repeat sequences flanking the SCC*mec* amplification may also suggest that an initial double-strand break (DSB), followed by RecA-dependent DSB repair during rolling circle replication may drive the production of long tandem arrays in a single generation, which have previously been implicated in fast adaption to drug treatment (21). Following the initial SCC*mec* duplication/amplification, the long stretches of homology are likely to facilitate RecA-mediated expansion and contraction of the element in different concentrations of oxacillin, as recently observed in a *S. lugdenensis* strain carrying an amplified *isd* locus (16). Recombination events leading to partial deletion of the SCC*mec* locus have been described previously. For instance, increased vancomycin resistance has

been linked to site-specific insertion sequence-mediated excision of SCC*mec* (22), suggesting that distinct RecA-independent mechanisms may favour high or low copy numbers of *mecA* in high β-lactam or vancomycin environments, respectively.

Even though multiple copies of SCC*mec* were maintained by HoR34 following repeated subculture in the absence of oxacillin selection, no evidence for SCC*mec* amplification was found in a search of 404 MRSA genomes using read coverage of the *mecA* gene normalised with read coverage of three single copy genes (data not shown). The clinical relevance of this data merits further investigation, particularly given that β-lactams are not typically part of the treatment regimen for MRSA infections. However, this may change in view of ongoing clinical trials showing the therapeutic value of combining flucloxacillin and vancomycin for the treatment of MRSA sepsis (23, 24). Our growth competition experiments revealed the increased competitiveness of HoR34 in the presence of oxacillin was balanced by a significant loss of competitiveness in the absence of antibiotic selection, suggesting that MRSA strains carrying multiple SCC*mec* elements are unlikely to be maintained under physiological conditions or in clinical environments where exposure to antibiotics is sporadic. Taken together our data identify chromosomal amplification of the SCC*mec* element as a new mechanism that may be used by MRSA to adapt to, and be more competitive in, high oxacillin environments.

232 **Materials and Methods**

233 **Strains and culture conditions.** Strains used in this study are listed in Table 2 and were
234 grown at 37°C in LB (Sigma), BHI (Oxoid), Mueller Hinton (Oxoid) or nutrient (Oxoid) broth
235 supplemented with ampicillin (50 μg/ml), oxacillin (0.5, 64, 100 or 130 μg/ml),
236 chloramphenicol (10 μg/ml) or erythromycin (10 μg/ml) as indicated. *S. aureus* strains were
237 also grown on BHI agar media plates supplemented with oxacillin concentrations up to 1200
238 μg/ml.
239
240 **Measurement of oxacillin minimum inhibitory concentration (MIC).** The oxacillin MIC for
241 the *S. aureus* strains used in this study was determined in accordance with the Clinical
242 Laboratory Standards Institute (CLSI) guidelines and using E-tests strips from Biomerieux on
243 Mueller Hinton agar (Oxoid) containing 2% NaCl.
244
245 **Isolation of USA300 oxacillin hyper-resistant mutants using chemostat system.** The
246 community-associated CA-MRSA strain, USA300 FPR3757, which expresses a HeR
247 phenotype with an oxacillin minimum inhibitory concentration (MIC) on brain heart infusion
248 or nutrient agar of 32 μg/ml was used in this study. A 580 ml capacity laboratory reactor
249 containing 500 ml of nutrient broth (Oxoid) was used as described previously (25). USA300
250 was inoculated into the chemostat and allowed to grow to stationary phase for 2 days at
251 37^{o}C in the absence of any antibiotic selection or media replacement. A growth media
252 reservoir containing 20 l of nutrient broth was then connected to the chemostat and fed to
253 the chemostat using a peristaltic pump at a flow rate of 100 ml/h, replacing the entire
254 nutrient broth volume of the chemostat every 5h. After 24 hours continuous culture growth
255 in the absence of antibiotic selection, the nutrient broth in the feeding tank was
256 supplemented with oxacillin at a concentration of 8 mg/l. Thereafter the oxacillin
257 concentration in the growth medium reservoir was increased in a step-wise manner every
258 day reaching a final concentration of 130 mg/l on Day 12. Culture samples were collected
259 aseptically from the chemostat after 24 hours culture at each oxacillin concentration before
260 being serially diluted and inoculated onto BHI agar supplemented with oxacillin 100 μg/ml.
261 The MICs of colonies recovered from these plates were determined on BHI agar
262 supplemented with oxacillin ranging from 100-1000 μg/ml. All isolates examined were

hyper-resistant and capable of robust growth on BHI agar supplemented with 800 μg/ml oxacillin. Phenotypic and whole genome sequence analysis of the hyper-resistant mutants is described in the supplementary methods.

Haemolysis, biofilm and autolysis assays. Beta haemolysis was assessed on BHI agar supplemented with 5% sheep blood following overnight growth at 37°C and a further 24 hours at 4°C. Semi-quantitative measurements of biofilm formation were determined under static conditions using Nunclon Hydrophilic tissue culture treated 96 well polystyrene plates (Nunc, Denmark) as described previously (26). Triton X-100 induced autolysis was measured essentially as described previously (27). Each experiment was repeated at least three times and average data presented.

Transmission Electron Microscopy (TEM). Overnight BHI cultures were diluted 1:200 in fresh BHI and grown at 37°C to an A_{600} = 1.0. 10 ml culture aliquots were subjected to centrifugation at 8,000 × *g*, and the cell pellets were re-suspended in fixation solution (2.5% glutaraldehyde in 0.1 M cacodylate buffer [pH 7.4]) and incubated overnight at 4°C. The fixed cells were further treated with 2% osmium tetroxide, followed by 0.25% uranyl acetate for contrast enhancement. The pellets were then dehydrated in increasing concentrations of ethanol as described above for the SEM cell preparation, followed by pure propylene oxide, and transferred to a series of resin and propylene oxide mixtures (50:50, 75:25, pure resin) before being embedded in Epon resin. Thin sections were cut on an ultramicrotome. Images were analysed using AMT v.542 software using a Hitachi H7000 instrument. At least 3 to 5 measurements of cell wall thickness were performed on each cell and 88 cells were measured for each sample.

PCR and Quantitative PCR. Amplification of the *mecA* gene and the SCC*mec* junctions in HoR34 was achieved using the following primers (Table 3): mecA_Fwd and mecA_Rev (for *mecA*) and SCCmecJNFwd and SCCmecJnRev (for the SCC*mec* junctions). Quantitative PCR (qPCR) for *mecA* was performed on the Roche LightCycler 480 instrument using the LightCycler 480 Sybr Green Kit (Roche) and the following primers: mecA1_Fwd and mecA2_Rev. Cycling conditions were 95 °C for 5 minutes and followed by 45 cycles of 95 °C for 10 seconds, 58 °C for 20 seconds and 72°C for 20 seconds. Melt curve analysis was

performed at 95 °C for 5 seconds followed by 65 °C for one minute up to 97 °C at a ramp rate of 0.11c/sec with five readings taken for every degree of temperature increase. The *gyrB* gene was used as an internal standard for all reactions using previous described primers (2). For each reaction, the ratio of *mecA* and *gyrB* transcript number was calculated as follows: $2^{(Ct\ gyrB\ -\ Ct\ mecA)}$. Each qPCR experiment was performed at least three times and average data and standard errors are presented.

Analysis of PBP2a expression: Total cell protein preparations were prepared from overnight cultures grown in 0, 0.5, 64 or 100 µg/ml oxacillin. Cell pellets were re-suspended in distilled water containing 5 µg/ml lysostaphin, 10 units of DNase I, and 50 µl of 10% SDS before being incubated at 37°C for 30 minutes. Insoluble material was pelleted by centrifugation and the supernatant used for Western blotting. Protein concentration was assessed using the Pierce BCA protein assay kit (Thermo Scientific). Protein samples were separated on a 10% SDS gel (Thermo Scientific) and transferred to nitrocellulose membranes (Thermo Scientific) using a TE 70 semidry transfer unit (Amersham). Anti-PBP2a antibodies (Abnova) were used at a 1:2000 dilution. A 1:200 dilution of protein G-horseradish peroxidase (HRP) conjugate (Sigma) was used to detect bound antibody and visualisation was achieved using a colorimetric detection system (Bio-Rad).

Complementation of HoR34 with *gdpP, guaA, camS* and *clpX*. The *gdpP, guaA, camS* and *clpX* genes were amplified from USA300 genomic DNA by PCR using primers listed in Table 2, before being cloned into the cloning vector pDrive (Quigen) in *Escherichia coli* TOP10. The sequence of inserts in recombinant plasmids was verified by Sanger sequencing (Source Biosciences) before being subcloned on *Eco*RI or *Bam*HI/*Hin*dIII restriction fragments into the *E. coli* - *Staphylococcus* shuttle plasmid pLI50. The plasmids were transformed by electroporation into the restriction-deficient strain RN4220, and subsequently into HoR34. All plasmid-harbouring strains were cultured in medium supplemented with 100 µg/ml ampicillin (*E. coli*) or 10 µg/ml chloramphenicol (*S. aureus*) for plasmid selection.

Growth competition experiments. Overnight cultures of USA300 and HoR34 cultures were diluted to A_{600} = 0.05 in fresh BHI media and grown for 6h. The cell density of both exponential phase cultures was adjusted to A_{600} = 0.1 in 500 ml flasks containing 50ml BHI or BHI supplemented with 0.5 µg/ml oxacillin and incubated at 37°C with shaking. The number

of colony forming units in samples collected at 0, 2, 4, 8, 24 and 48h was determined by plating serial dilutions on BHI agar. Colonies formed by each strain were readily differentiated based on their tetracycline resistance and appearance i.e. the HoR34 colonies were tetracycline sensitive and had a white-coloured, small colony phenotype whereas USA300 colonies were regular sized, tetracycline resistant and pigmented.

Statistical analysis. Two-tailed, two-sample equal variance Student's t-Tests were used to determine statistically significant differences in assays performed during this study. A *P* value <0.05 was deemed significant.

Quality control of genome sequence data. Read quality was assessed by screening the read length, nucleotide and quality score distributions using FastQC (http://www.bioinformatics.babraham.ac.uk/projects/fastqc/) and the FASTX-Toolkit (http://hannonlab.cshl.edu/fastx_toolkit/index.html). The DNA reads were trimmed based on quality scores. Potential adaptor sequence was removed using Trimmomatic v0.32 (28), which scanned reads using a four-base sliding window and trimmed reads where the average Phred base quality of the window was below 30. All ambiguous 'N' bases and reads shorter than 35 bp were removed. The first 20 bases of the DNA reads were removed because they had a nucleotide content that deviated from the expected 25% rate for each base. The DNA reads were corrected using BayesHammer (29) to reduce sequencing errors that can reduce the alignment quality, increase false positive SNP rates and reduce the number of valid SNPs (30). These steps retained 84% of the initial DNA reads among HoR isolates from the chemostat yielding median quality values > 30 across the reads. Insert sizes were an average of 185. Read lengths after trimming and filtering averaged 185 bp and the average coverage per sample on the chromosome, calculated using the Bedtools genomecov function (31) on mapped reads, ranged from 47 to 197.

Genome assembly. The error-corrected paired and unpaired reads for each DNA sample were assembled using SPAdes v3.1.1 [5] with k-mers 21, 33, 55, 77, 99 and 127 and the 'careful' parameter, which minimized the number of mismatches in the contigs (32). The resulting assemblies were compared to the reference USA300_FPR3757 (PMID:16517273) chromosome using QUAST v2.3 (33). The GC content of each assembly was 32.6%, and there

were between 31 and 51 scaffolds per assembly, with N50 values > 200 Kb. One or two short gaps (<500 bp) were found in each assembly that could not be fully closed using Gapfiller (34).

Single nucleotide polymorphism (SNP) calling using assembly and read-mapping. The chromosome and three plasmids (GenBank accessions NC_007790-NC_007793) were indexed with *k*-mer of thirteen and step size of two using SMALT v5.7 (http://www.sanger.ac.uk/science/tools/smalt-0). The error-corrected DNA reads were mapped to the genome with SMALT, which applied a Smith-Waterman sequence alignment algorithm. The SAM (sequence alignment/map) files were converted to BAM (binary alignment/map) files using Samtools v0.1.18 (35). The BAM files were then coordinate-sorted, the paired and unpaired files were merged, and PCR duplicate reads were removed. Candidate SNPs were detected where the base quality (BQ) was >25, the mapping quality (MQ) was >30, and the read depth was <100 using Samtools Mpileup v0.1.18, Bcftools v0.1.17-dev, and the Samtools v0.1.11 vcfutils.pl function. The read depth allele frequency of the non-reference allele (RDAF) and local coverage were estimated using Samtools Pileup v0.1.11.

To call SNPs using an assembly-based approach, the scaffolds produced by SPAdes were aligned to the USA300 reference genome using nucmer in the MUMmer v3.23 package. This was followed by eliminating conflicting repeat copies using the 'delta-filter' command and the 'show-snps' comand to call SNPs and indels. The union of SNPs called by nucmer and SNPs called by Bcftools was used as a candidate SNP set. These sites were queried across all samples using the Samtools Pileup files to find false negative SNPs uncalled by nucmer or Bcftools. The RDAF of the non-reference alleles was reported for each SNP using Samtools Pileup output. Each candidate SNP was assessed using the following additional criteria:

1) SNP Quality (SQ) >30
2) read coverage >5
3) forward-reverse read coverage ratio between 0.1 and 0.9
4) non-reference read allele frequency >0.1
5) 2+ forward reads

389 6) 2+ reverse reads

390 Results were converted to variant call format (VCF) and annotated. SNPs were homozygous
391 if the RDAF was ≥ 0.85 and heterozygous if 0.1 < RDAF < 0.85. Insufficient read depth
392 coverage was present to predict SNPs with RDAF < 0.1.

393 **Indel calling using split-read mapping.** Deletions and short insertions (indels) were called
394 using the samtopindel script to convert the BAM files, and then with Pindel (36) to only keep
395 indels with at least ten supporting reads. The RDAF of the indels smaller than the read
396 length were calculated using the BAM files in IGV (number of reads with indel at locus / all
397 reads at the locus). For indels greater than one bp in length, the sum of the number of reads
398 with the indel was divided by the sum of the number of reads at each site in the indel. This
399 approach may be limited by uneven coverage at a locus. If the indel was longer than the
400 read length, then a lack of read coverage at the sites predicted to have the mutation was
401 considered evidence of the deletion and the RDAF was set to one.

402 **Variant annotation.** The functional effect of SNPs and indels was estimated by annotation
403 with SnpEff v4.0e (37) using the 'Staphylococcus_aureus_USA300_FPR3757_uid58555'
404 database file from the SnpEff database. Results were manually checked using the reference
405 genome annotation.

406 **Copy number variation detection using read coverage.** Copy number variants (CNVs) were
407 screened using the BAM files containing reads with MQ > 30 to reduce false positive rates
408 [12–14]. Coverage was calculated for every base using genomecov in Bedtools with the '-d'
409 flag (31) so that the median chromosomal coverage could be calculated for each sample.
410 Genome-wide coverage levels were analysed in 10 Kb and 25 Kb windows and plotted as 5
411 Kb sliding windows with a 2.5 Kb step using the Bedtools makewindows function (31).
412 Coverage for each window was normalised by dividing it by the median coverage of the
413 chromosome to produce a copy number estimate. Windows with copy number ≥ 2 were
414 reported. The copy number of plasmids was determined by dividing the median read
415 coverage of the plasmid by the median read coverage of the chromosome.

416 **MinION long-read genome sequencing.** To evaluate the number of SCCmec copies and their
417 location contiguous with or excised from the chromosome, genomic DNA from HoR34 was

amplified to generate long reads using a Oxford Nanopore Technologies (ONT) MinION. MinION sequencing library construction was carried out according to manufacturer's instructions and as previously described (38). The library was sequenced on an R7.3 MinION flowcell using the 2D sequencing protocol. The run produced 26859 FAST5 files, which were processed using poRe (39), yielding 17254 2D reads. These reads were used with the MiSeq data in a hybrid assembly using SPAdes (32) and SSPACE-LongRead (40) to produce a single contig.

Figure Legends

Figure 1. Growth and cell morphology phenotypes of USA300 and HoR34. A. Small colony variants and other isolates recovered from the chemostat culture after 13 days at a final oxacillin concentration of 130 mg/l grown on BHI agar for 24 h. **B.** Growth curve of USA300 and HoR34 grown for 20 hours in BHI media at 37^{o}C with vigorous aeration. The number of colony forming units per ml in culture samples removed at regular intervals was determined by plating on BHI agar. **C.** Cell morphology of USA300 and HoR34 imaged using transmission electron microscopy (TEM) at 8,000× magnification. **D.** Cell wall thickness of USA300 and HoR34 determined using TEM at 100,000× magnification and AMT v.542 imaging software.

Figure 2. Oxacillin susceptibility and autolysis phenotypes of USA300 and HoR34. A. Oxacillin MIC of USA300, HoR34 and HoR34 carrying plasmids pLI50 (control), p*gdpP*, p*guaA* and p*camS* determined using Etests. **B.** Autolytic activity in USA300 and HoR34. USA300, HoR34, HoR34 carrying plasmids pLI50 (control), p*gdpP*, p*guaA* and p*camS*, and a USA300 JE2 *atl* mutant (negative control) were grown to early exponential phase in BHI at 37°C and washed in PBS and adjusted to A_{600} = 1.0 in 0.01% Triton X-100. The A_{600} was measured initially and at 15 min intervals thereafter with shaking incubation at 37°C. Autolytic activity is expressed as a percentage of the initial A_{600}. Average results from three independent experiments shown.

Figure 3. Copy number as determined by Illumina sequence read coverage across SCC*mec* for USA300 (Sample 1A_S1), HoR34 (Sample 8A_S8, highlighted with blue box) and eight other isolates from the chemostat culture. The position on the chromosome is indicated, with SCC*mec* coordinates between 0.034 and 0.057 Mb. The blue lines depict locally weighted scatterplot smoothing (lowess) applied to the data points (black). Note that the y-axis for HoR34 differs from the other samples.

Figure 4. Chromosomal organisation of HoR34 depicting expansion of the SCC*mec* element and locations of *gdpP, clpX, camS* and *guaA* mutations. On the circular map, the inner track shows copy number of 10 kb non-overlapping loci across the genome with loci that had copy number greater than two shown in red and those with copy number less than two

shown in blue. The next track shows black blocks illustrating different regions on the genome e.g. SCC*mec* and ACME. Single nucleotide polymorphisms are shown on the third track. Missense mutations are labelled in green whereas stop gain mutations are labelled in blue. Genes are shown in the outermost tracks. Genes transcribed in the forward (5' -> 3') direction are labelled in green and are in the outside track whereas those transcribed in the reverse direction are labelled in red.

Figure 5. Chromosomal amplification of SCC*mec* can drive high level oxacillin resistance. A. PCR amplification across the SCC*mec* junctions in HoR34. Amplification of the *mecA* gene in both USA300 and HoR34 was used as a control. **B.** Comparison of relative *mecA* abundance by LightCycler qPCR in USA300 and HoR34 grown for 24 h in BHI supplemented with 0, 0.5, 64 or 100 mg/ml oxacillin. **C.** Comparison of relative PBP2a expression by Western blot analysis in USA300 and HoR34 grown in BHI and BHI supplemented with 0, 0.5, 64 or 100 mg/ml oxacillin. **D.** Competitive growth of USA300 and HoR34 over 48 hours in BHI and BHI supplemented with oxacillin (0.5 mg/ml). The CFU of each strain was enumerated on BHI agar to count all bacteria and BHI oxacillin (30 mg/ml) to count HoR34. The ratio of the two strains in each culture is shown. The data presented are mean and SD of three experiments. Statistical evaluation was performed using a paired two tailed t-test.

481 **Acknowledgements.** This study was funded by grants from the Irish Health Research Board
482 (HRA-POR-2012-51 and HRA-POR-2015-1158) (to J.P.O'G). We thank Cyril Carroll and Claire
483 Fingleton for assistance with the chemostat experiment and analysis of HoR34.

484 **Table 1. Genetic alterations in USA300 oxacillin hyper-resistant mutants from the**
485 **chemostat culture**

Isolate, growth chafracteristic	Genome position	Nucleotide change	Amino acid change	Locus tag/gene
HoR20, fast-growing	703854	G-C	$Glu_{227}Gln$	RS03375/*abcA*
HoR18, 21, 27, 36; fast-growing	110748, 110752,111618, 111630, 111648	Multiple	Multiple	RS00520-RS00525 /uncharacterized lipoprotein genes
HoR33, 41, 43, 46; fast-growing	2288896	G-A	$Ser_{67}Lys$	RS11640/*dacA*
HoR34, slow-growing	19122	A-C	$Thr_{260}Pro$	*gdpP* (c-di-AMP phosphodiesterase (14))
	44078	C-T	$Ala_{314}Val$	*guaA* (GMP synthetase (9))
	441379	G-T	$Glu_{511}Asp$	*guaA*
	1775825	C-A	$Glu_{37}STOP$	*clpX* (Chaperone with ClpP-dependent role in protein degradation and ClpP-independent role in protein folding (10))
	2046530	G-A	$Gln_{305}STOP$	*camS* (membrane lipoprotein involve in sex pheromone biosynthesis (11))

486

487

488 **Table 2. Bacterial strains and plasmids used in this study**

Strains/plasmids	Relevant Details
S. aureus	
RN4220	Restriction-deficient laboratory *S. aureus.*
USA300	CA-MRSA expressing heterogeneous resistance to oxacillin
HoR34	USA300 derivative expressing high level resistance to oxacillin
ATCC 29213	MSSA strain for susceptibility testing
JE2 *atl*::*erm*	Transposon mutation in the major autolysin gene *atl* of strain JE2, a USA300 derivate used in the construction of the Nebraska Transposon mutant library (41). Exhibits impaired autolytic activity.
E. coli	*E. coli* Top10 cloning strain.
Plasmids	
pLI50	*E. coli-Staphylococcus* shuttle vector. Ap^r (*E. coli*), Cm^r (*Staphylococcus*).
pDrive	*E. coli* cloning vector

489
490
491
492

493 **Table 3. Oligonucleotide primers used in this study**

Target Gene	Primer Name	Primer Sequence (5'-3')
gdpP	gdpP_Fwd	GCCGAATGCAGTAACGATTT
	gdpP_Rev	TTGTTGGCGTTCTTGTTTTG
guaA	guaA_Fwd	AGAGGACAAAGCGCCTAAGA
	guaA_Rev	CCTTACCCCTTTTCCGTCCT
clpX	clpX_Fwd	AACGCAAAGTTCGTTGAAGG
	clpX_Rev	TGAGCGTCAACTTTGATTGG
camS	camS_Fwd	GCTGGTGAAGATGCAGGTTC
	camS_Rev	CCTGGTGCATTTGTTGAAACTG
mecA	mecA_Fwd	CATATCGTGAGCAATGAACTGA
	mecA_Rev	CATCGTTACGGATTGCTTCA
SCCmec Junction	SCCmecJn_Fwd	CTTGCTGGGTGCTATTTGA
	SCCmecJn_Rev	CGCTGTCTTCCTGTATTTCG
mecA	mecA1_Fwd	TGCTCAATATAAAATTAAAACAAACTACGGTAAC
	mecA1_Rev	GAATAATGACGCTATGATCCCAA
gyrB	gyrB_Fwd	CCAGGTAAATTAGCCGATTGC
	gyrB_Rev	AAATCGCCTGCGTTCTAGAG

494
495

References

1. **Bal AM, Coombs GW, Holden MT, Lindsay JA, Nimmo GR, Tattevin P, Skov RL.** 2016. Genomic insights into the emergence and spread of international clones of healthcare-, community- and livestock-associated meticillin-resistant Staphylococcus aureus: Blurring of the traditional definitions. J Glob Antimicrob Resist **6:**95-101.
2. **Pozzi C, Waters EM, Rudkin JK, Schaeffer CR, Lohan AJ, Tong P, Loftus BJ, Pier GB, Fey PD, Massey RC, O'Gara JP.** 2012. Methicillin resistance alters the biofilm phenotype and attenuates virulence in Staphylococcus aureus device-associated infections. PLoS Pathog **8:**e1002626.
3. **Andersson DI, Levin BR.** 1999. The biological cost of antibiotic resistance. Curr Opin Microbiol **2:**489-493.
4. **Gagneux S, Long CD, Small PM, Van T, Schoolnik GK, Bohannan BJ.** 2006. The competitive cost of antibiotic resistance in Mycobacterium tuberculosis. Science **312:**1944-1946.
5. **Sieradzki K, Tomasz A.** 1997. Suppression of beta-lactam antibiotic resistance in a methicillin-resistant Staphylococcus aureus through synergic action of early cell wall inhibitors and some other antibiotics. J Antimicrob Chemother **39 Suppl A:**47-51.
6. **Dengler V, McCallum N, Kiefer P, Christen P, Patrignani A, Vorholt JA, Berger-Bachi B, Senn MM.** 2013. Mutation in the C-di-AMP cyclase dacA affects fitness and resistance of methicillin resistant Staphylococcus aureus. PLoS One **8:**e73512.
7. **Dordel J, Kim C, Chung M, Pardos de la Gandara M, Holden MT, Parkhill J, de Lencastre H, Bentley SD, Tomasz A.** 2014. Novel determinants of antibiotic resistance: identification of mutated loci in highly methicillin-resistant subpopulations of methicillin-resistant Staphylococcus aureus. MBio **5:**e01000.
8. **Domanski TL, de Jonge BL, Bayles KW.** 1997. Transcription analysis of the Staphylococcus aureus gene encoding penicillin-binding protein 4. J Bacteriol **179:**2651-2657.
9. **Mulhbacher J, Brouillette E, Allard M, Fortier LC, Malouin F, Lafontaine DA.** 2010. Novel riboswitch ligand analogs as selective inhibitors of guanine-related metabolic pathways. PLoS Pathog **6:**e1000865.
10. **Baek KT, Bowman L, Millership C, Dupont Sogaard M, Kaever V, Siljamaki P, Savijoki K, Varmanen P, Nyman TA, Grundling A, Frees D.** 2016. The Cell Wall Polymer Lipoteichoic Acid Becomes Nonessential in Staphylococcus aureus Cells Lacking the ClpX Chaperone. MBio **7**.
11. **Shahmirzadi SV, Nguyen MT, Gotz F.** 2016. Evaluation of Staphylococcus aureus Lipoproteins: Role in Nutritional Acquisition and Pathogenicity. Front Microbiol **7:**1404.
12. **Proctor RA, Kriegeskorte A, Kahl BC, Becker K, Loffler B, Peters G.** 2014. Staphylococcus aureus Small Colony Variants (SCVs): a road map for the metabolic pathways involved in persistent infections. Front Cell Infect Microbiol **4:**99.
13. **Baek KT, Grundling A, Mogensen RG, Thogersen L, Petersen A, Paulander W, Frees D.** 2014. beta-Lactam resistance in methicillin-resistant Staphylococcus aureus USA300 is increased by inactivation of the ClpXP protease. Antimicrob Agents Chemother **58:**4593-4603.

14. **Corrigan RM, Abbott JC, Burhenne H, Kaever V, Grundling A.** 2011. c-di-AMP is a new second messenger in Staphylococcus aureus with a role in controlling cell size and envelope stress. PLoS Pathog **7:**e1002217.
15. **Gao W, Monk IR, Tobias NJ, Gladman SL, Seemann T, Stinear TP, Howden BP.** 2015. Large tandem chromosome expansions facilitate niche adaptation during persistent infection with drug-resistant Staphylococcus aureus. Microbial Genomics **1**.
16. **Heilbronner S, Monk IR, Brozyna JR, Heinrichs DE, Skaar EP, Peschel A, Foster TJ.** 2016. Competing for Iron: Duplication and Amplification of the isd Locus in Staphylococcus lugdunensis HKU09-01 Provides a Competitive Advantage to Overcome Nutritional Limitation. PLoS Genet **12:**e1006246.
17. **Diep BA, Stone GG, Basuino L, Graber CJ, Miller A, des Etages SA, Jones A, Palazzolo-Ballance AM, Perdreau-Remington F, Sensabaugh GF, DeLeo FR, Chambers HF.** 2008. The arginine catabolic mobile element and staphylococcal chromosomal cassette mec linkage: convergence of virulence and resistance in the USA300 clone of methicillin-resistant Staphylococcus aureus. J Infect Dis **197:**1523-1530.
18. **Higgins PG, Rosato AE, Seifert H, Archer GL, Wisplinghoff H.** 2009. Differential expression of ccrA in methicillin-resistant Staphylococcus aureus strains carrying staphylococcal cassette chromosome mec type II and IVa elements. Antimicrob Agents Chemother **53:**4556-4558.
19. **Mir-Sanchis I, Roman CA, Misiura A, Pigli YZ, Boyle-Vavra S, Rice PA.** 2016. Staphylococcal SCCmec elements encode an active MCM-like helicase and thus may be replicative. Nat Struct Mol Biol **23:**891-898.
20. **Lovett ST, Drapkin PT, Sutera VA, Jr., Gluckman-Peskind TJ.** 1993. A sister-strand exchange mechanism for recA-independent deletion of repeated DNA sequences in Escherichia coli. Genetics **135:**631-642.
21. **Sandegren L, Andersson DI.** 2009. Bacterial gene amplification: implications for the evolution of antibiotic resistance. Nat Rev Microbiol **7:**578-588.
22. **Noto MJ, Fox PM, Archer GL.** 2008. Spontaneous deletion of the methicillin resistance determinant, mecA, partially compensates for the fitness cost associated with high-level vancomycin resistance in Staphylococcus aureus. Antimicrob Agents Chemother **52:**1221-1229.
23. **Tong SY, Nelson J, Paterson DL, Fowler VG, Jr., Howden BP, Cheng AC, Chatfield M, Lipman J, Van Hal S, O'Sullivan M, Robinson JO, Yahav D, Lye D, Davis JS, group Cs, the Australasian Society for Infectious Diseases Clinical Research N.** 2016. CAMERA2 - combination antibiotic therapy for methicillin-resistant Staphylococcus aureus infection: study protocol for a randomised controlled trial. Trials **17:**170.
24. **Davis JS, Sud A, O'Sullivan MV, Robinson JO, Ferguson PE, Foo H, van Hal SJ, Ralph AP, Howden BP, Binks PM, Kirby A, Tong SY, Combination Antibiotics for MRSasg, Australasian Society for Infectious Diseases Clinical Research N.** 2016. Combination of Vancomycin and beta-Lactam Therapy for Methicillin-Resistant Staphylococcus aureus Bacteremia: A Pilot Multicenter Randomized Controlled Trial. Clin Infect Dis **62:**173-180.
25. **Fleming GTA, Patching JW.** 2008. The Fermenter in Research and Development. Wiley, Chichester, England.

26. **Conlon KM, Humphreys H, O'Gara JP.** 2002. icaR encodes a transcriptional repressor involved in environmental regulation of ica operon expression and biofilm formation in Staphylococcus epidermidis. J Bacteriol **184:**4400-4408.
27. **McCarthy H, Waters EM, Bose JL, Foster S, Bayles KW, O'Neill E, Fey PD, O'Gara JP.** 2016. The major autolysin is redundant for Staphylococcus aureus USA300 LAC JE2 virulence in a murine device-related infection model. FEMS Microbiol Lett **363:**fnw087.
28. **Bolger AM, Lohse M, Usadel B.** 2014. Trimmomatic: a flexible trimmer for Illumina sequence data. Bioinformatics **30:**2114-2120.
29. **Nikolenko SI, Korobeynikov AI, Alekseyev MA.** 2013. BayesHammer: Bayesian clustering for error correction in single-cell sequencing. BMC Genomics **14 Suppl 1:**S7.
30. **Kelley DR, Schatz MC, Salzberg SL.** 2010. Quake: quality-aware detection and correction of sequencing errors. Genome Biol **11:**R116.
31. **Quinlan AR, Hall IM.** 2010. BEDTools: a flexible suite of utilities for comparing genomic features. Bioinformatics **26:**841-842.
32. **Bankevich A, Nurk S, Antipov D, Gurevich AA, Dvorkin M, Kulikov AS, Lesin VM, Nikolenko SI, Pham S, Prjibelski AD, Pyshkin AV, Sirotkin AV, Vyahhi N, Tesler G, Alekseyev MA, Pevzner PA.** 2012. SPAdes: a new genome assembly algorithm and its applications to single-cell sequencing. J Comput Biol **19:**455-477.
33. **Gurevich A, Saveliev V, Vyahhi N, Tesler G.** 2013. QUAST: quality assessment tool for genome assemblies. Bioinformatics **29:**1072-1075.
34. **Boetzer M, Pirovano W.** 2012. Toward almost closed genomes with GapFiller. Genome Biol **13:**R56.
35. **Li H, Handsaker B, Wysoker A, Fennell T, Ruan J, Homer N, Marth G, Abecasis G, Durbin R, Genome Project Data Processing S.** 2009. The Sequence Alignment/Map format and SAMtools. Bioinformatics **25:**2078-2079.
36. **Ye K, Schulz MH, Long Q, Apweiler R, Ning Z.** 2009. Pindel: a pattern growth approach to detect break points of large deletions and medium sized insertions from paired-end short reads. Bioinformatics **25:**2865-2871.
37. **Cingolani P, Platts A, Wang le L, Coon M, Nguyen T, Wang L, Land SJ, Lu X, Ruden DM.** 2012. A program for annotating and predicting the effects of single nucleotide polymorphisms, SnpEff: SNPs in the genome of Drosophila melanogaster strain w1118; iso-2; iso-3. Fly (Austin) **6:**80-92.
38. **Risse J, Thomson M, Patrick S, Blakely G, Koutsovoulos G, Blaxter M, Watson M.** 2015. A single chromosome assembly of Bacteroides fragilis strain BE1 from Illumina and MinION nanopore sequencing data. Gigascience **4:**60.
39. **Watson M, Thomson M, Risse J, Talbot R, Santoyo-Lopez J, Gharbi K, Blaxter M.** 2015. poRe: an R package for the visualization and analysis of nanopore sequencing data. Bioinformatics **31:**114-115.
40. **Boetzer M, Pirovano W.** 2014. SSPACE-LongRead: scaffolding bacterial draft genomes using long read sequence information. BMC Bioinformatics **15:**211.
41. **Fey PD, Endres JL, Yajjala VK, Widhelm TJ, Boissy RJ, Bose JL, Bayles KW.** 2013. A genetic resource for rapid and comprehensive phenotype screening of nonessential Staphylococcus aureus genes. MBio **4:**e00537-00512.

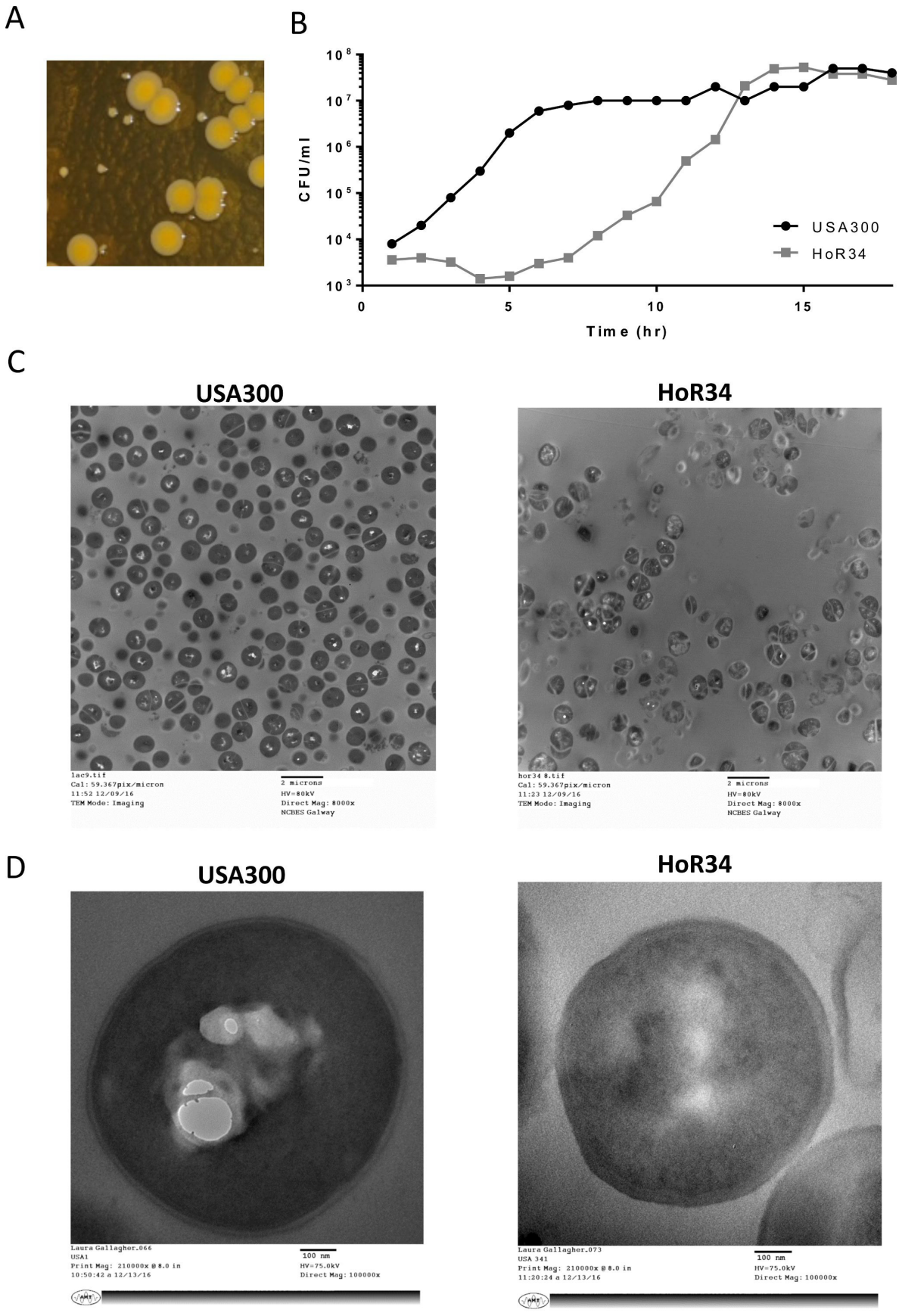

Fig. 1

A

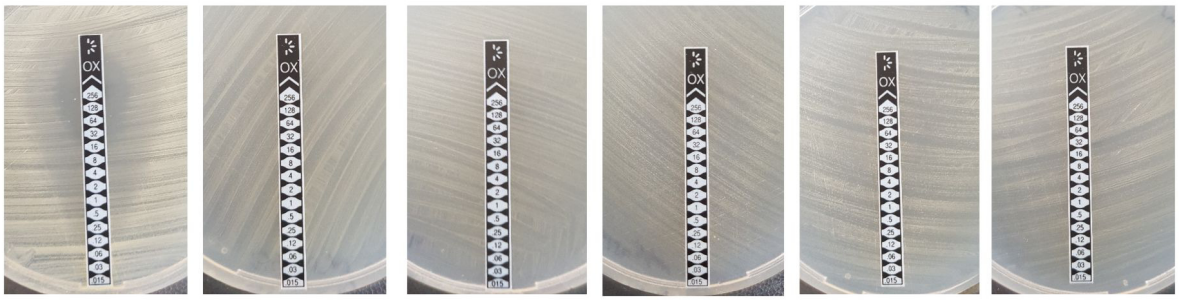

B

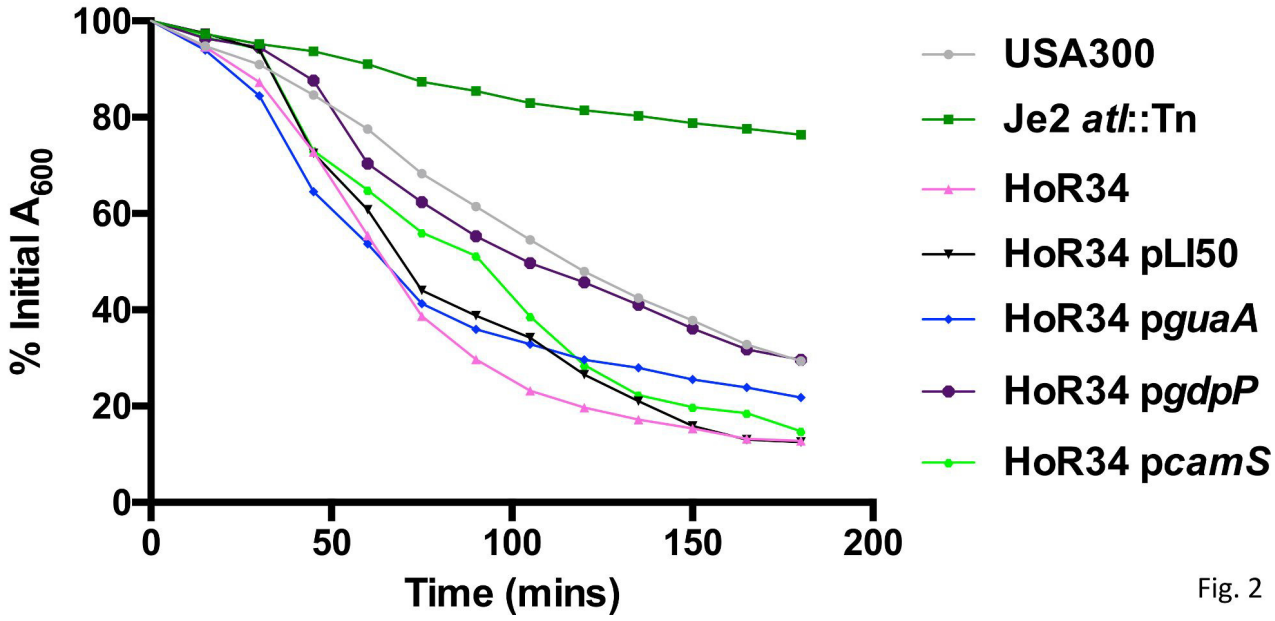

Fig. 2

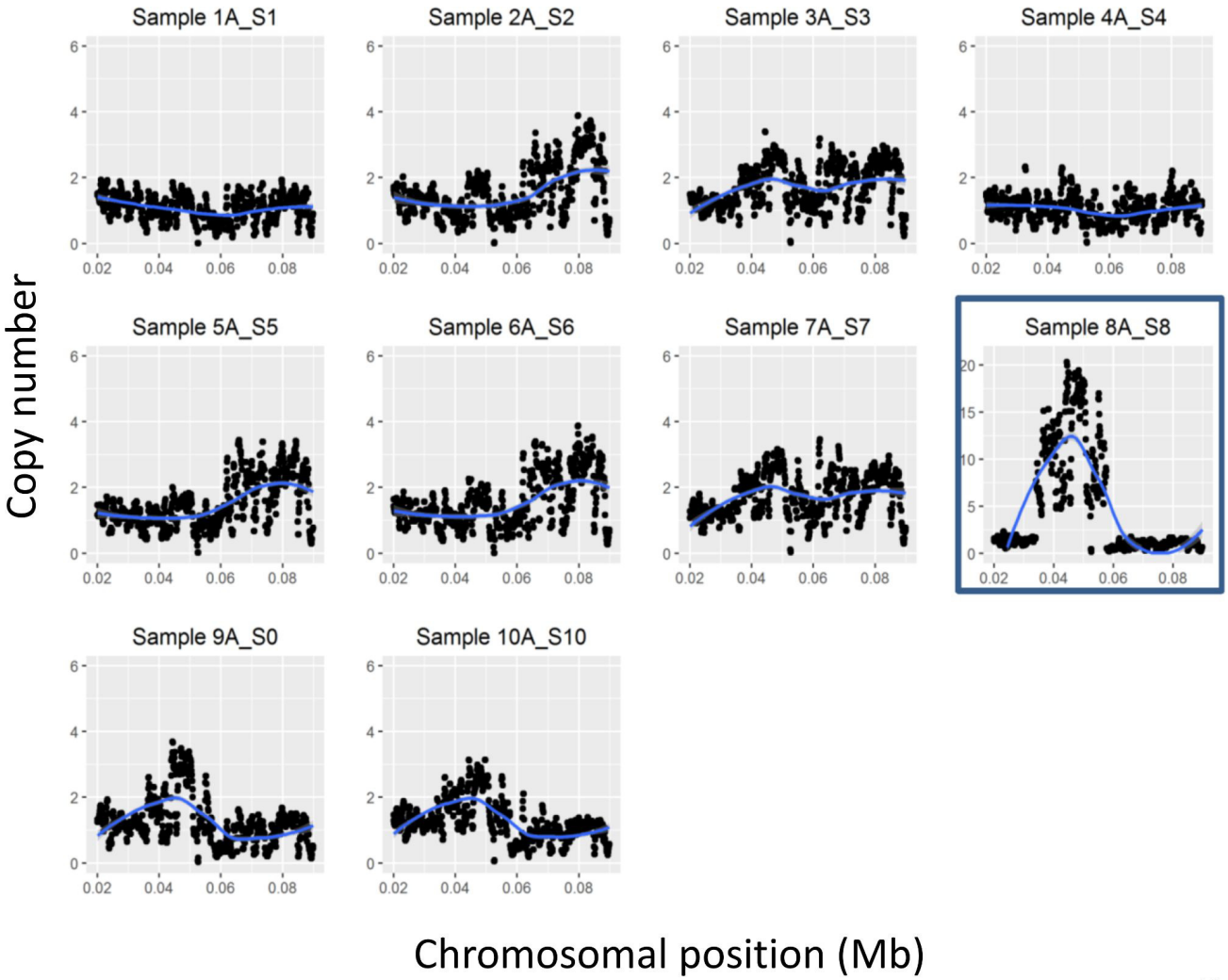

Fig. 3

Antimicrobial Agents and Chemotherapy

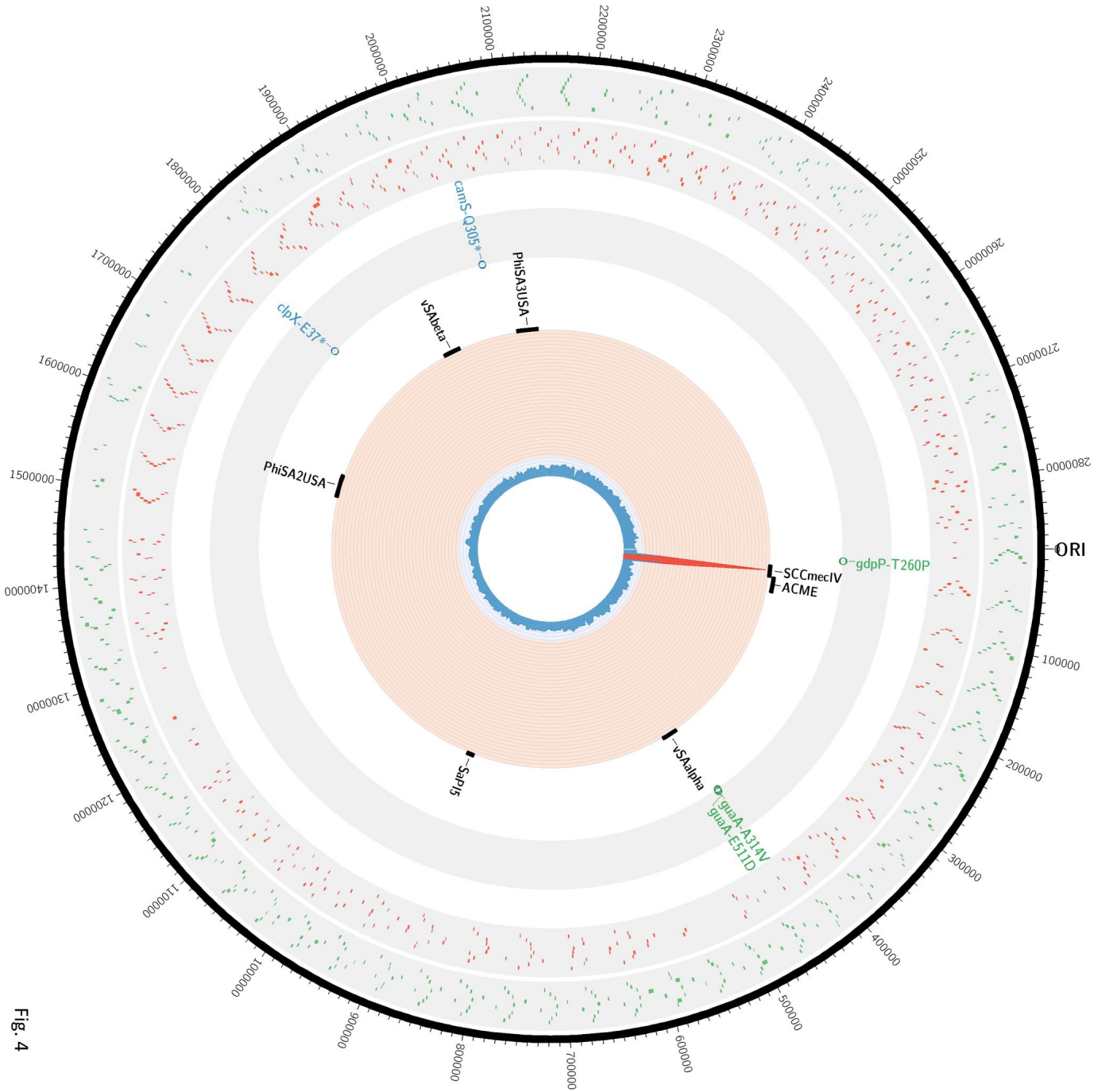

Fig. 4

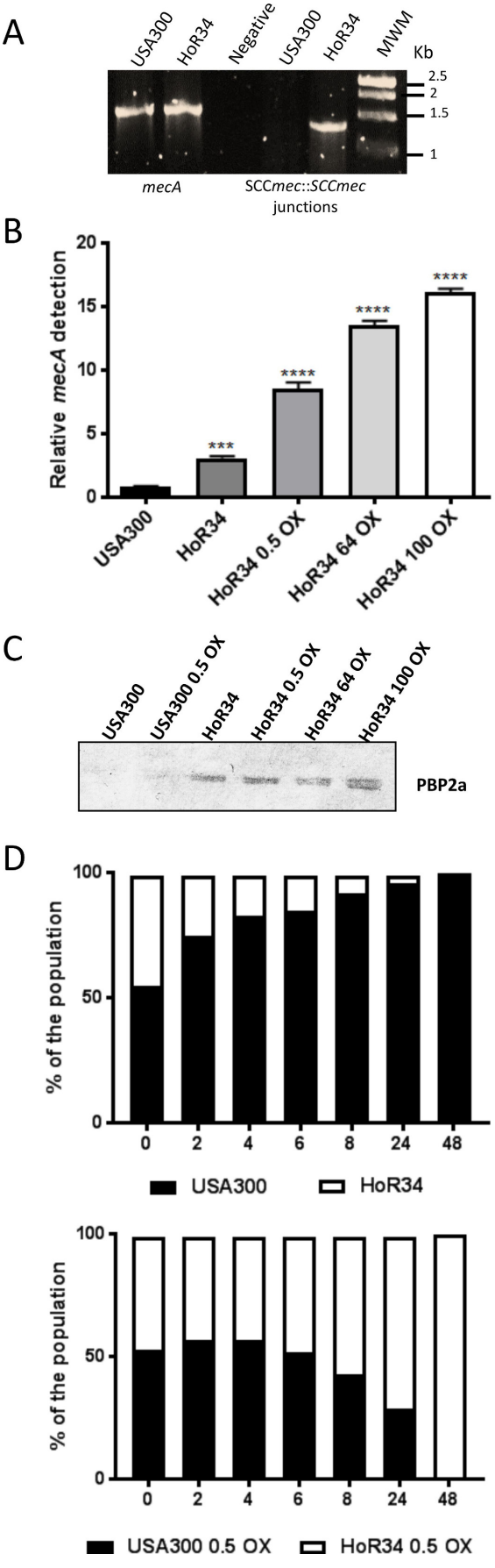

Fig. 5